

$B_s \rightarrow D_s(3040)$ form factors and B_s decays into $D_s(3040)$ Gang Li ^{a *}, Feng-Lan Shao ^{a †} and Wei Wang ^{b ‡}^a *Department of Physics, Qufu Normal University, Shandong 273165, People's Republic of China*^b *Istituto Nazionale di Fisica Nucleare, Sezione di Bari, Bari 70126, Italy*

Under the assignment of $D_s(3040)$ as a radially excited p-wave $\bar{c}s$ state with $J^P = 1^+$, we compute the $B_s \rightarrow D_s(3040)$ form factors within the covariant light-front quark model. Two classification schemes for the p-wave $\bar{c}s$ meson are adopted. We also use our results to predict the branching ratios (BRs), polarization fractions, and angular asymmetries in semileptonic $B_s \rightarrow D_s(3040)\ell\bar{\nu}(\ell = e, \mu, \tau)$. The BRs are found at the order of 10^{-3} for $\ell = e, \mu$, and 10^{-5} for $\ell = \tau$. We find that the polarization fractions and angular asymmetries could be useful to pin down the ambiguities in theoretical prescriptions for $D_s(3040)$. In addition, we investigate the nonleptonic $B_s \rightarrow D_s(3040)M$ decays under the factorization method, where M denotes a charged pseudoscalar or a vector meson. The BRs of $B_s \rightarrow D_s(3040)\rho$ and $B_s \rightarrow D_s(3040)D_s^*$ reach the order of 10^{-3} , while the other channels are typically smaller by 1-2 orders.

PACS numbers: 12.39.Ki; 13.20.He; 13.25.Hw

I. INTRODUCTION

The observations of a number of new resonances, such as the narrow states $D_s(2317)$ in the $D_s^+\pi^0$ final state and $D_s(2460)$ in the $D_s^*\pi^0$ and $D_s\gamma$ channel [1, 2], have brought great opportunities for our understanding of nonperturbative QCD in the charm mass region. They also initiate tremendous efforts on the exploration of exotic hadrons beyond the naive quark model and revive great interests in the study of the $c\bar{s}$ spectrum [3].

In the heavy quark limit, the heavy quark will decouple from the light degrees of freedom and act as a static color source. Strong interactions will be independent of the heavy flavor and spin. In this case, heavy-light mesons, the eigenstates of the QCD Lagrangian in the heavy quark limit, can be labeled according to the total angular momentum s_l of the light degrees of freedom. Heavy mesons with the same s_l but different spin orientations of the heavy quark fill into one doublet. Accordingly, heavy mesons can be classified by these doublets, characterized by s_l instead of the commonly-used quantum numbers, $^{2S+1}L_J$.

The classification scheme based on the heavy quark symmetry applies to the D_{sJ} mesons. For instance, $D_s(1969)$ and $D_s^*(2112)$ can be arranged into the lowest-lying doublet with $J_{s_l}^P = (0^-, 1^-)_{1/2}$. Among the p-wave $c\bar{s}$ states, $D_{s0}(2317)$ and $D_{s1}(2460)$ belong to the doublet with $J_{s_l}^P = (0^+, 1^+)_{1/2}$, and doublet $J_{s_l}^P = (1^+, 2^+)_{3/2}$ can be filled by $D_{s1}(2536)$ and $D_{s2}(2573)$. Despite some controversies over their internal structures, these mesons have been well established in experiment.

Several other resonant signals have also been observed recently on the B factories and other facilities. The SELEX collaboration reported one narrow state $D_{sJ}(2632)$ in 2004 [4], which however, has not been confirmed so far by other experiments. $D_s(2710)$ is announced in B meson decays by the Belle collaboration [5] and also confirmed by the BaBar results [6]. The $D_s(2860)$ is discovered in the DK final state by BaBar [7]. Recently, the BaBar collaboration has reported one new D_{sJ} state in the study of the e^+e^- annihilations [6]. The mass and decay width of this broad state are

$$m = (3044 \pm 8_{-5}^{+30})\text{MeV}, \quad \Gamma = (239 \pm 35_{-42}^{+46})\text{MeV}. \quad (1)$$

Its quantum numbers could be $J^P = 0^-, 1^+, 2^- \dots$, taking into account its signal in D^*K instead of DK . The angular analysis is not available because of the limited statistics.

During the past few years, some progresses have been made in the classification of these states and understanding of their peculiar properties in the production or decay processes. Towards this direction, if the 3^- assignment of $D_s(2710)$ [8–10] is confirmed by the data (see Ref. [11] for an alternative scenario), the $D_s(3040)$ would be unfavored to be 2^- since the mass inversion seems unlikely. On the other hand, the 1^+ assignment is favored in several aspects.

* Email:gli@mail.ihep.ac.cn

† Email:shaoff@mail.sdu.edu.cn

‡ Email:wwang@mail.ihep.ac.cn

Firstly, this explanation is supported by the study of the spectroscopy of excited D_s mesons [12–14], though predictions in Refs. [15, 16] are lower than the experimental value by roughly 200 MeV. Reference [10] investigates these new D_{sJ} mesons in a semi-classic flux tube model and concludes that $D_s(3040)$ is compatible with the 1^+ assignment. The authors of Ref. [17] have studied the strong decays of $D_s(3040)$ with four different assignments, and find that the decay width with $J^P = 1^+$ is also consistent with the value given by BaBar. The strong decays of $D_s(3040)$ are also investigated in the 3P_0 constituent quark model [18] and chiral quark model [19], respectively.

The verification of the above new states can be via not only the analysis of their decay properties, which have been widely discussed in the literature, but also via their productions, which so far have not been investigated in detail. The production processes of the above mentioned new states in B_s decays would be an ideal way of probing their properties. Productions of $D_s(2317)$ and $D_s(2460)$ in the B_s decays have received some theoretical attentions [22–26]. On the experimental side, a large number of B_s events will be collected by the LHCb [20] and forthcoming Super B factory experiment [21]. From the theoretical viewpoint, the degrees of freedom over the m_b scale in B_s decays can be computed in the perturbation theory and the evolution between the m_W and m_b can be organized using the renormalization group. The low-energy effects, which are parameterized into hadronic form factors, will then probe the structures of the D_{sJ} mesons.

To proceed, we will study the $B_s \rightarrow D_{sJ}$ form factors and the production rates of D_{sJ} mesons in semileptonic and nonleptonic B_s decays in the framework of a covariant light-front quark model (LFQM) [27]. This approach is suitable for handling the heavy-light mesons and has been successfully applied to various processes [28–33]. In particular, we will focus on the $D_s(3040)$ with its assignment as a $2P$ state. The $B_s \rightarrow D_s^*$ transition form factors will be extracted as a byproduct.

This paper is organized as follows. In the next section, an introduction to the light-front quark model and expressions for the transition form factors between the B_s and $(D_s^*, D_s(3040))$ mesons are presented. In Sec. III, we compute the form factors under two different assignments for the $D_s(3040)$. With the form factors at hand, we will explore in Sec. IV the semileptonic B_s decays and the nonleptonic $B_s \rightarrow D_s(3040)$ decays under the factorization assumption. The last section contains our conclusions.

II. FORM FACTORS IN THE COVARIANT LFQM

In the effective electroweak Hamiltonian responsible for $B_s \rightarrow D_{sJ} l \bar{\nu}$ [34]

$$H_{\text{eff}} = \frac{G_F}{\sqrt{2}} V_{cb} [\bar{c} \gamma_\mu (1 - \gamma_5) b] [\bar{l} \gamma^\mu (1 - \gamma_5) \nu], \quad (2)$$

G_F and V_{cb} are the Fermi constant and the Cabibbo-Kobayashi-Maskawa (CKM) matrix element, respectively. The leptonic part can be directly calculated using perturbation theory. The residual part contains hadronic effects and will be incorporated into the transition form factors as

$$\begin{aligned} \langle D_s^*(P'', \varepsilon'') | V_\mu | \bar{B}_s(P') \rangle &= -\frac{1}{m_{B_s} + m_{D_s^*}} \epsilon_{\mu\nu\alpha\beta} \varepsilon''^{\nu} P^\alpha q^\beta V^{B_s D_s^*}(q^2), \\ \langle D_s^*(P'', \varepsilon'') | A_\mu | \bar{B}_s(P') \rangle &= i \left\{ (m_{B_s} + m_{D_s^*}) \varepsilon''^{\mu} A_1^{B_s D_s^*}(q^2) - \frac{\varepsilon''^* \cdot P}{m_{B_s} + m_{D_s^*}} P_\mu A_2^{B_s D_s^*}(q^2) \right. \\ &\quad \left. - 2m_{D_s^*} \frac{\varepsilon''^* \cdot P}{q^2} q_\mu [A_3^{B_s D_s^*}(q^2) - A_0^{B_s D_s^*}(q^2)] \right\}, \\ \langle D_{s1}(P'', \varepsilon'') | A_\mu | \bar{B}_s(P') \rangle &= -\frac{i}{m_{B_s} - m_{D_{s1}}} \epsilon_{\mu\nu\alpha\beta} \varepsilon''^{\nu} P^\alpha q^\beta A^{B_s D_{s1}}(q^2), \\ \langle D_{s1}(P'', \varepsilon'') | V_\mu | \bar{B}_s(P') \rangle &= -\left\{ (m_{B_s} - m_{D_{s1}}) \varepsilon''^{\mu} V_1^{B_s D_{s1}}(q^2) - \frac{\varepsilon''^* \cdot P}{m_{B_s} - m_{D_{s1}}} P_\mu V_2^{B_s D_{s1}}(q^2) \right. \\ &\quad \left. - 2m_{D_{s1}} \frac{\varepsilon''^* \cdot P}{q^2} q_\mu [V_3^{B_s D_{s1}}(q^2) - V_0^{B_s D_{s1}}(q^2)] \right\}, \end{aligned} \quad (3)$$

where $P = P' + P''$, $q = P' - P''$, and the convention $\epsilon_{0123} = 1$ is adopted. The vector and axial-vector currents are defined as $\bar{c} \gamma_\mu b$ and $\bar{c} \gamma_\mu \gamma_5 b$. We have adopted the 1^+ assignment, denoted as D_{s1} hereafter, for the $D_s(3040)$ meson. In the subsequent analysis two kinds of axial-vectors ($^{2S+1}L_J = ^3P_1$ or 1P_1) will be considered, and for short we will also abbreviate them as 3A and 1A , respectively. To smear the singularity at $q^2 = 0$, we obtain the constraints on the

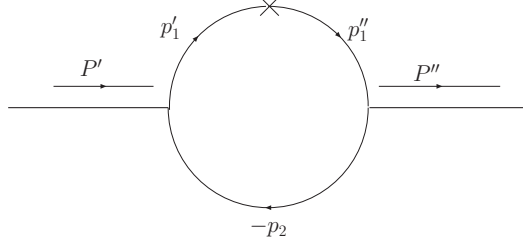


FIG. 1: Feynman diagram for a transition form factor, where the cross symbol denotes the electroweak vertex.

form factors $A_3^{B_s D_s^*}(0) = A_0^{B_s D_s^*}(0)$ and $V_3^{B_s D_{s1}}(0) = V_0^{B_s D_{s1}}(0)$, where

$$A_3^{B_s D_s^*}(q^2) = \frac{m_{B_s} + m_{D_s^*}}{2m_{D_s^*}} A_1^{B_s D_s^*}(q^2) - \frac{m_{B_s} - m_{D_s^*}}{2m_{D_s^*}} A_2^{B_s D_s^*}(q^2), \quad (4)$$

$$V_3^{B_s D_{s1}}(q^2) = \frac{m_{B_s} - m_{D_{s1}}}{2m_{D_{s1}}} V_1^{B_s D_{s1}}(q^2) - \frac{m_{B_s} + m_{D_{s1}}}{2m_{D_{s1}}} V_2^{B_s D_{s1}}(q^2). \quad (5)$$

To be specific, we will compute these transition form factors by considering the general $P \rightarrow V$ and $P \rightarrow A$ transitions, where A denotes either 3P_1 or 1P_1 state. The LFQM is based on the light-front field theory, where the plus component of the gluon degrees of freedom vanishes in the light-cone gauge. In this framework, it is convenient to use the light-front decomposition of the momentum $P' = (P'^-, P'^+, P'_\perp)$, with $P'^\pm = P'^0 \pm P'^3$, so that $P'^2 = P'^+ P'^- - P'^2_\perp$. The incoming (outgoing) meson has the momentum of $P' = p'_1 + p_2$ ($P'' = p''_1 + p_2$) and mass of M' (M''). The quark and antiquark inside the incoming (outgoing) meson have the mass m'_1 (m_2). Their momenta are denoted as p'_1 (p_2), respectively. In particular, these momenta can be expressed in terms of the internal variables (x_i, p'_\perp)

$$p'_{1,2}{}^+ = x_{1,2} P'^+, \quad p'_{1,2\perp} = x_{1,2} P'_\perp \pm p'_\perp, \quad (6)$$

with $x_1 + x_2 = 1$. Using these internal variables, one can define some useful quantities for the incoming meson

$$\begin{aligned} M_0'^2 &= (e'_1 + e'_2)^2 = \frac{p_\perp'^2 + m_1'^2}{x_1} + \frac{p_\perp'^2 + m_2^2}{x_2}, & \widetilde{M}_0' &= \sqrt{M_0'^2 - (m'_1 - m_2)^2}, \\ e_i^{(\prime)} &= \sqrt{m_i^{(\prime)2} + p_\perp'^2 + p_z'^2}, & p_z' &= \frac{x_2 M_0'}{2} - \frac{m_2^2 + p_\perp'^2}{2x_2 M_0'}, \end{aligned} \quad (7)$$

where e_i can be interpreted as the energy of the quark or the antiquark, and M_0' is the kinetic invariant mass of the meson system. One advantage of these internal quantities is that they are Lorentz invariant. The definition of the internal quantities for the outgoing meson is similar. To formulate the amplitude for the transition form factor, we also require the Feynman rules for the meson-quark-antiquark vertices ($i\Gamma'_M$)

$$\begin{aligned} i\Gamma'_P &= H'_P \gamma_5, \\ i\Gamma'_V &= iH'_V [\gamma_\mu - \frac{1}{W'_V} (p'_1 - p_2)_\mu], \\ i\Gamma'_{3A} &= iH'_{3A} [\gamma_\mu + \frac{1}{W'_{3A}} (p'_1 - p_2)_\mu] \gamma_5, \\ i\Gamma'_{1A} &= iH'_{1A} [\frac{1}{W'_{1A}} (p'_1 - p_2)_\mu] \gamma_5. \end{aligned} \quad (8)$$

In the case of the outgoing meson, we shall use $i(\gamma_0 \Gamma_M^\dagger \gamma_0)$ for the relevant vertices.

The lowest order contribution to a form factor is depicted in Fig. 1, in which the cross label in the diagram denotes the V , A transition vertex. In B_s to D_{sJ} decays, p'_1 (p''_1) is the momentum of the bottom (charm) quark, while p_2 is the momentum of the antiquark. Physical quantities, e.g. decay constants and form factors, can be expressed in terms of Feynman momentum loop integrals which are manifestly covariant. As an example, we consider the $P \rightarrow V$ transition

$$\mathcal{B}_\mu^{PV} = -i^3 \frac{N_c}{(2\pi)^4} \int d^4 p'_1 \frac{H'_P(iH''_V)}{N'_1 N''_1 N_2} S_{\mu\nu}^{PV} \varepsilon^{\prime*\nu}, \quad (9)$$

where $N_1'^{(\prime\prime)} = p_1'^{(\prime\prime)2} - m_1'^{(\prime\prime)2}$ and $N_2 = p_2^2 - m_2^2$ arise from the quark propagators and $N_c = 3$ is the color factor. The function $S_{\mu\nu}^{PV}$ is from the Lorentz contraction of the propagators and the vertex functions

$$\begin{aligned} S_{\mu\nu}^{PV} &= (S_V^{PV} - S_A^{PV})_{\mu\nu} \\ &= \text{Tr} \left[\left(\gamma_\nu - \frac{1}{W_V''} (p_1'' - p_2)_\nu \right) (\not{p}_1'' + m_1'') (\gamma_\mu - \gamma_\mu \gamma_5) (\not{p}_1' + m_1') \gamma_5 (-\not{p}_2 + m_2) \right]. \end{aligned} \quad (10)$$

The form factors will be obtained by evaluating the above formulas. In practice, we perform the integration over the minus component within the contour method. If the covariant vertex functions are not singular when perform the integration, the amplitude will pick up the singularities in the antiquark propagator. This manipulation then leads to

$$\begin{aligned} N_1'^{(\prime\prime)} &\rightarrow \hat{N}_1'^{(\prime\prime)} = x_1 (M'^{(\prime\prime)2} - M_0'^{(\prime\prime)2}), \\ H_M'^{(\prime\prime)} &\rightarrow h_M'^{(\prime\prime)}, \\ W_M'' &\rightarrow w_M'', \\ \int \frac{d^4 p_1'}{N_1' N_1'' N_2} H_P' H_V'' S^{PV} &\rightarrow -i\pi \int \frac{dx_2 d^2 p_\perp'}{x_2 \hat{N}_1' \hat{N}_1''} h_P' h_V'' \hat{S}^{PV}, \end{aligned} \quad (11)$$

where

$$M_0''^2 = \frac{p_\perp'^2 + m_1'^2}{x_1} + \frac{p_\perp'^2 + m_2^2}{x_2} \quad (12)$$

with $p_\perp'' = p_\perp' - x_2 q_\perp$. The explicit forms of h_M' and w_M' used in this work are given by [27, 28]

$$\begin{aligned} h_P' &= h_V' = (M'^2 - M_0'^2) \sqrt{\frac{x_1 x_2}{N_c}} \frac{1}{\sqrt{2} \hat{M}_0'} \varphi', \\ \sqrt{\frac{2}{3}} h_{3A}' &= (M'^2 - M_0'^2) \sqrt{\frac{x_1 x_2}{N_c}} \frac{1}{\sqrt{2} \hat{M}_0'} \frac{\hat{M}_0'^2}{2\sqrt{3} \hat{M}_0'} \varphi_p', \\ h_{1A}' &= (M'^2 - M_0'^2) \sqrt{\frac{x_1 x_2}{N_c}} \frac{1}{\sqrt{2} \hat{M}_0'} \varphi_p', \\ w_{3A}' &= \frac{\hat{M}_0'^2}{m_1' - m_2}, \quad w_{1A}' = 2, \end{aligned} \quad (13)$$

where φ' and φ_p' are the light-front wave functions for the s-wave and p-wave mesons, respectively.

One difference between the conventional LFQM [35–38] and the covariant LFQM lies in the treatment of the constituent quarks. In the conventional LFQM, the constituent quarks are required to be on mass shell. Physical quantities can be extracted from the plus component of the current matrix elements. However, this framework suffers from the non-covariance problem arising from the missing zero-mode contributions. This drawback is resolved by including the so-called Z -diagram. In the covariant LFQM the quarks and antiquarks are off-shell and the physical quantities are written as the integration over the 4-momentum of the antiquark. The conventional LFQM will be recovered after the integration over the minus component, where the antiquark is set on-shell. The Lorentz covariance would be lost again as it receives additional contributions proportional to the light-like four vector $\tilde{\omega} = (0, 2, \mathbf{0}_\perp)$. This is spurious since the vector never appears in the definition of the form factors. The advantage of the covariant LFQM is that we can directly handle the non-covariant terms instead of compute the Z -diagram. Specifically, the spurious terms can be eliminated by performing the p^- integration in a proper way and the corresponding rules are derived in Refs. [27, 28]. The above manipulation results in the expression for $P \rightarrow V$ form factors:

$$g(q^2) = -\frac{N_c}{16\pi^3} \int dx_2 d^2 p_\perp' \frac{2h_P' h_V''}{x_2 \hat{N}_1' \hat{N}_1''} \left\{ x_2 m_1' + x_1 m_2 + (m_1' - m_1'') \frac{p_\perp' \cdot q_\perp}{q^2} + \frac{2}{w_V''} \left[p_\perp'^2 + \frac{(p_\perp' \cdot q_\perp)^2}{q^2} \right] \right\},$$

$$\begin{aligned}
f(q^2) &= \frac{N_c}{16\pi^3} \int dx_2 d^2 p'_\perp \frac{h'_P h''_V}{x_2 \hat{N}'_1 \hat{N}''_1} \left\{ 2x_1(m_2 - m'_1)(M_0'^2 + M_0''^2) - 4x_1 m''_1 M_0'^2 + 2x_2 m'_1 q \cdot P \right. \\
&\quad + 2m_2 q^2 - 2x_1 m_2 (M'^2 + M''^2) + 2(m'_1 - m_2)(m'_1 + m''_1)^2 + 8(m'_1 - m_2) \left[p_\perp'^2 + \frac{(p'_\perp \cdot q_\perp)^2}{q^2} \right] \\
&\quad + 2(m'_1 + m''_1)(q^2 + q \cdot P) \frac{p'_\perp \cdot q_\perp}{q^2} - 4 \frac{q^2 p_\perp'^2 + (p'_\perp \cdot q_\perp)^2}{q^2 w_V''} \left[2x_1 (M'^2 + M_0'^2) - q^2 - q \cdot P \right. \\
&\quad \left. \left. - 2(q^2 + q \cdot P) \frac{p'_\perp \cdot q_\perp}{q^2} - 2(m'_1 - m''_1)(m'_1 - m_2) \right] \right\}, \\
a_+(q^2) &= \frac{N_c}{16\pi^3} \int dx_2 d^2 p'_\perp \frac{2h'_P h''_V}{x_2 \hat{N}'_1 \hat{N}''_1} \left\{ (x_1 - x_2)(x_2 m'_1 + x_1 m_2) - [2x_1 m_2 + m''_1 + (x_2 - x_1)m'_1] \frac{p'_\perp \cdot q_\perp}{q^2} \right. \\
&\quad \left. - 2 \frac{x_2 q^2 + p'_\perp \cdot q_\perp}{x_2 q^2 w_V''} \left[p'_\perp \cdot p''_\perp + (x_1 m_2 + x_2 m'_1)(x_1 m_2 - x_2 m''_1) \right] \right\}, \\
a_-(q^2) &= \frac{N_c}{16\pi^3} \int dx_2 d^2 p'_\perp \frac{h'_P h''_V}{x_2 \hat{N}'_1 \hat{N}''_1} \left\{ 2(2x_1 - 3)(x_2 m'_1 + x_1 m_2) - 8(m'_1 - m_2) \left[\frac{p_\perp'^2}{q^2} + 2 \frac{(p'_\perp \cdot q_\perp)^2}{q^4} \right] \right. \\
&\quad - [(14 - 12x_1)m'_1 - 2m''_1 - (8 - 12x_1)m_2] \frac{p'_\perp \cdot q_\perp}{q^2} \\
&\quad + \frac{4}{w_V''} \left([M'^2 + M''^2 - q^2 + 2(m'_1 - m_2)(m''_1 + m_2)](A_3^{(2)} + A_4^{(2)} - A_2^{(1)}) \right. \\
&\quad + Z_2(3A_2^{(1)} - 2A_4^{(2)} - 1) + \frac{1}{2}[x_1(q^2 + q \cdot P) - 2M'^2 - 2p'_\perp \cdot q_\perp - 2m'_1(m''_1 + m_2) \\
&\quad \left. \left. - 2m_2(m'_1 - m_2)](A_1^{(1)} + A_2^{(1)} - 1)q \cdot P \left[\frac{p_\perp'^2}{q^2} + \frac{(p'_\perp \cdot q_\perp)^2}{q^4} \right] (4A_2^{(1)} - 3) \right] \right\}, \tag{14}
\end{aligned}$$

with

$$\begin{aligned}
V^{B_s D_s^*}(q^2) &= -(m_{B_s} + m_{D_s^*}) g(q^2), \quad A_1^{B_s D_s^*}(q^2) = -\frac{f(q^2)}{m_{B_s} + m_{D_s^*}}, \\
A_2^{B_s D_s^*}(q^2) &= (m_{B_s} + m_{D_s^*}) a_+(q^2), \quad A_3^{B_s D_s^*}(q^2) - A_0^{B_s D_s^*}(q^2) = \frac{q^2}{2m_{D_s^*}} a_-(q^2). \tag{15}
\end{aligned}$$

The functions Z_2 , $A_1^{(1)}$, $A_2^{(1)}$, $A_3^{(2)}$, and $A_4^{(2)}$ are given in the Appendix.

The computation of $B_s \rightarrow D_s(3040)$ transition is analogous, and in fact, the $B \rightarrow^3 A$ form factors are related to the $B \rightarrow V$ ones. In particular, the auxiliary form factors are given as

$$\begin{aligned}
\ell^3 A(q^2) &= f(q^2) \text{ with } (m''_1 \rightarrow -m''_1, h''_V \rightarrow h''_{3A}, w''_V \rightarrow w''_{3A}), \\
q^3 A(q^2) &= g(q^2) \text{ with } (m''_1 \rightarrow -m''_1, h''_V \rightarrow h''_{3A}, w''_V \rightarrow w''_{3A}), \\
c_\pm^3 A(q^2) &= a_\pm(q^2) \text{ with } (m''_1 \rightarrow -m''_1, h''_V \rightarrow h''_{3A}, w''_V \rightarrow w''_{3A}), \tag{16}
\end{aligned}$$

where the replacement of $m''_1 \rightarrow -m''_1$ does not apply to m''_1 in w'' and h'' , as it arises from the propagators and quark-antiquark-meson coupling vertex

$$\begin{aligned}
S_{\mu\nu}^{P^3 A} &= (S_V^{P^3 A} - S_A^{P^3 A})_{\mu\nu} \\
&= \text{Tr} \left[\left(\gamma_\nu - \frac{1}{W_{3A}''} (p''_1 - p_2)_\nu \right) \gamma_5 (\not{p}''_1 + m''_1) (\gamma_\mu - \gamma_\mu \gamma_5) (\not{p}'_1 + m'_1) \gamma_5 (-\not{p}_2 + m_2) \right] \\
&= -S_{\mu\nu}^{PV} |_{W_V'' \rightarrow W_{3A}'', m''_1 \rightarrow -m''_1}. \tag{17}
\end{aligned}$$

Then, the $B_s \rightarrow D_s(^3A)$ form factors can be expressed by

$$\begin{aligned} A^{B_s D_{s1}(^3A)}(q^2) &= -(m_{B_s} - m_{D_{s1}(^3A)}) q^3 A(q^2), \quad V_1^{B_s D_{s1}(^3A)}(q^2) = -\frac{\ell^3 A(q^2)}{m_{B_s} - m_{D_{s1}(^3A)}}, \\ V_2^{B_s D_{s1}(^3A)}(q^2) &= (m_{B_s} - m_{D_{s1}(^3A)}) c_+^3 A(q^2), \quad V_3^{B_s D_{s1}(^3A)}(q^2) - V_0^{B_s D_{s1}(^3A)}(q^2) = \frac{q^2}{2m_{D_{s1}(^3A)}} c_-^3 A(q^2). \end{aligned} \quad (18)$$

The analysis is similar for the 1A meson but only the w_A'' terms contribute in the transition form factors, stemming from the structures of meson-quark-antiquark coupling vertices shown in Eq. (8).

Before closing this section, it is worth mentioning that the identification of $D_s(3040)$ with either 3P_1 or 1P_1 configuration may be inappropriate. As discussed above, in the heavy quark limit the QCD Lagrangian is invariant under the heavy flavor and spin rotation. Thus, the heavy quark will decouple from the remanent part. One direct consequence is that the heavy mesons are not labeled by the quantum number $^{2S+1}L_J$ but by the total angular momentum s_l of the light quark degrees of freedom. Finite heavy quark mass corrections will break this symmetry, and mesons with the same spin-parity J^P will mix with each other. The relation between these two bases is

$$\begin{aligned} |P_1^{3/2}\rangle &= \sqrt{\frac{2}{3}} |^1P_1\rangle + \sqrt{\frac{1}{3}} |^3P_1\rangle, \\ |P_1^{1/2}\rangle &= \sqrt{\frac{1}{3}} |^1P_1\rangle - \sqrt{\frac{2}{3}} |^3P_1\rangle. \end{aligned} \quad (19)$$

As follows, we will compute the $B_s \rightarrow D_s(3040)$ form factors and make predictions for physical observables in the relevant B_s decays under these two schemes.

III. NUMERICAL RESULTS

Expressions for form factors shown in Eq. (14) involve the quark masses, hadron masses and the light front wave functions (LFWFs) φ' and φ'_p . The latter should be obtained by solving the relativistic Schrödinger equation. However, in practice a phenomenological wave function to describe the hadronic structure is preferred. In this work, we will use the simple Gaussian-type wave function which has been extensively adopted in the literature [28, 29]

$$\varphi' = \varphi'(x_2, p'_\perp) = 4 \left(\frac{\pi}{\beta'^2} \right)^{3/4} \sqrt{\frac{dp'_z}{dx_2}} \exp \left(-\frac{p'^2_z + p'^2_\perp}{2\beta'^2} \right), \quad \frac{dp'_z}{dx_2} = \frac{e'_1 e_2}{x_1 x_2 M'_0}. \quad (20)$$

Similarly for the $D_s(3040)$, as one of the $2P$ states, the wave function is given as

$$\varphi'_p = \varphi'_p(x_2, p'_\perp) = 4 \sqrt{\frac{2}{3}} \left(\frac{\pi}{\beta'^2} \right)^{3/4} \sqrt{\frac{2}{\beta'^2}} \sqrt{\frac{dp_z}{dx_2}} \exp \left(-\frac{p^2_\perp + p^2_z}{2\beta'^2} \right) \times \left(\frac{p^2_\perp + p^2_z}{\beta'^2} - \frac{3}{2} \right). \quad (21)$$

The constituent mass for a heavy quark is usually believed close to the current quark mass. Running quark masses for a charm and bottom quark in the $\overline{\text{MS}}$ renormalization scheme are constrained as [39]

$$m_b = (4.19^{+0.18}_{-0.06}) \text{GeV}, \quad m_c = (1.27^{+0.07}_{-0.09}) \text{GeV}, \quad (22)$$

while the corresponding pole masses (with one-loop anomalous dimension) are

$$m_b = (4.65^{+0.20}_{-0.07}) \text{GeV}, \quad m_c = (1.56^{+0.09}_{-0.11}) \text{GeV}, \quad (23)$$

with $\alpha_s(m_Z = 91.19 \text{GeV}) = 0.120$ [39] in the renormalization group evolution equation. The quark mass extracted from the $\Upsilon(1S)$ is

$$m_b = (4.67^{+0.18}_{-0.06}) \text{GeV}. \quad (24)$$

In a phenomenological approach such as the quark model used in this work, the constituent quark mass is chosen close to the above results.

As well known, the constituent mass of a light quark largely deviates from its current mass due to non-negligible contributions from gluon degrees of freedom. In this case, only phenomenological values can be employed, and in principle, they can be constrained within a global fit under a specific framework. In this work, we will employ the

values which are consistent with the previous studies in the covariant LQFM. In particular, the same values as in Ref. [28] will be adopted

$$m_c = (1.4 \pm 0.1)\text{GeV}, \quad m_b = (4.64 \pm 0.2)\text{GeV}, \quad m_s = (0.37 \pm 0.05)\text{GeV}, \quad (25)$$

where a comprehensive study on D, B transition form factors has been performed and many predictions are found in accordance with the experimental data. It is worth mentioning that Ref. [28] only gives the central value for the quark masses. But here we also include sizable uncertainties to estimate the sensitivity. The above values in Eq. (25) are also consistent with the results derived from the variational principle in the conventional LQFM [40].

The shape parameter β' , which describes the momentum distribution, is fixed by the meson's decay constant, of which the analytic expression is derived as

$$\begin{aligned} f_P &= \frac{N_c}{16\pi^3} \int dx_2 d^2 p'_\perp \frac{h'_P}{x_1 x_2 (M'^2 - M_0'^2)} 4(m'_1 x_2 + m_2 x'_1), \\ f_V &= \frac{N_c}{M' 4\pi^3} \int dx_2 d^2 p'_\perp \frac{h'_V}{x_1 x_2 (M'^2 - M_0'^2)} \times \left[m_1 m_2 - m_1^2 + x_1 M_0'^2 - p_\perp'^2 + \frac{p_\perp'^2}{w_V} (m_2 + m_1) \right]. \end{aligned} \quad (26)$$

For the B_s meson decay constant, we use the latest Lattice QCD result [41]:

$$f_{B_s} = (231 \pm 15)\text{MeV}. \quad (27)$$

The D_s decay constant can be measured by the semileptonic $D_s \rightarrow \mu \bar{\nu}_\mu$ decays, for which a number of measurements are available. The averaged value by the HFAG at 1σ level will be used in this work [42]

$$f_{D_s} = (256.9 \pm 6.8)\text{MeV}. \quad (28)$$

At present, no direct measurement of the D_s^* decay constant is available. Fortunately, the heavy quark symmetry (HQS) implies that this quantity can be related to f_{D_s} , i.e.

$$f_{D_s^*} = \sqrt{\frac{m_{D_s}}{m_{D_s^*}}} f_{D_s} = (248.0 \pm 6.6)\text{MeV}. \quad (29)$$

Symmetry breaking effects emerge as power corrections in Λ_{QCD}/m_Q (here Λ_{QCD} is the hadronic scale while m_Q can be chosen as m_c or m_{D_s, D_s^*}), of which the value can amount to 20%. In the present work, we will use the value derived from the HQS relation and neglect the power corrections. Using the above decay constants, we fix the shape parameters in the LFWFs as

$$\beta_{B_s} = (0.6224 \pm 0.0339)\text{GeV}, \quad \beta_{D_s^*} = (0.421 \pm 0.007)\text{GeV}. \quad (30)$$

With the instantaneous Bethe-Salpeter method, the decay constant for radially excited 1^+ states has been studied by Ref. [16], i.e.

$$f_{D_s(2^3 P_1)} = 204\text{MeV}, \quad f_{D_s(2^1 P_1)} = 50\text{MeV}, \quad (31)$$

but no uncertainties can be found in Ref. [16]. With the value for $f_{D_s(2^3 P_1)}$ and identifying $D_s(3040)$ as one $2^3 P_1$ state, we find that the shape parameter is close to 0.3 GeV. As a first step to proceed, we will employ this value with an uncertainty as follows,

$$\beta_{D_s(3040)} = (0.300 \pm 0.015)\text{GeV}. \quad (32)$$

This choice corresponds to the decay constant

$$f_{D_s(2^3 P_1)} = (198^{+20}_{-21})\text{MeV}, \quad f_{D_s(2^1 P_1)} = (58 \pm 5)\text{MeV}. \quad (33)$$

For later convenience, the decay constants of D^- extracted from the experimental data of $D^- \rightarrow \mu^- \bar{\nu}$, and D^{*-} from HQS are also listed:

$$f_D = (216.6 \pm 17.2)\text{MeV}, \quad f_{D^*} = \sqrt{\frac{m_D}{m_{D^*}}} f_D = (209.1 \pm 16.8)\text{MeV}. \quad (34)$$

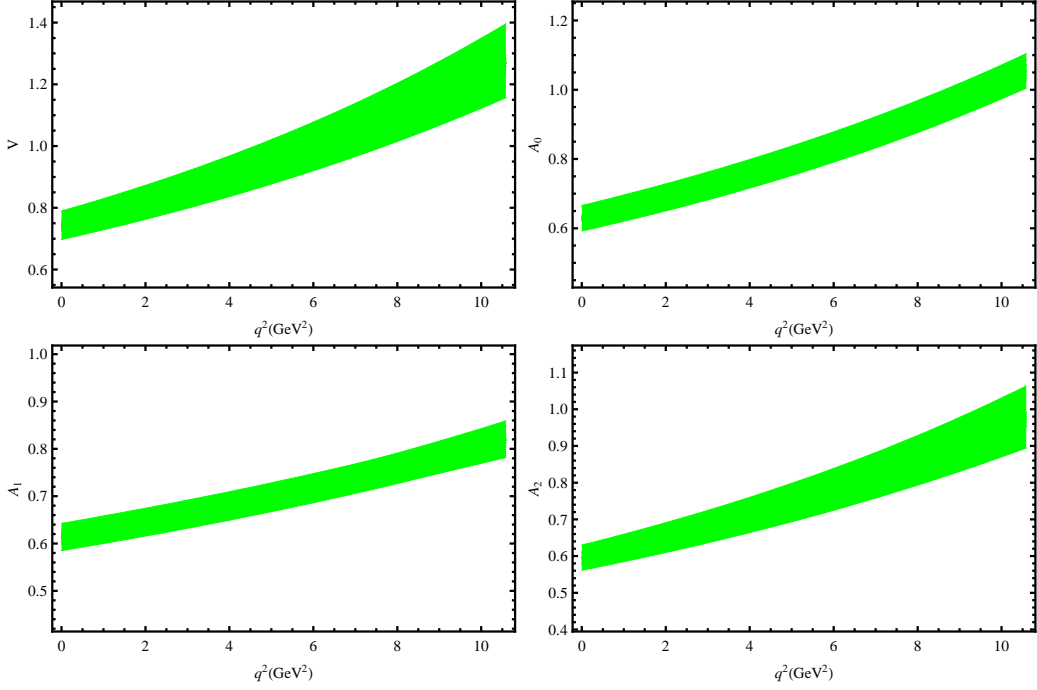


FIG. 2: The q^2 -dependence of the $B_s \rightarrow D_s^*$ form factors

Decay constants of the light mesons are obtained by making use of the experimental data of $P \rightarrow l\bar{\nu}$ and $\tau \rightarrow V^-\nu_\tau$ decays [39]

$$f_\pi = 0.131\text{GeV}, \quad f_K = 0.16\text{GeV}, \quad f_\rho = 0.2212\text{GeV}, \quad f_{K^*} = 0.2068\text{GeV}. \quad (35)$$

It is worth pointing out that because of the condition $q^+ = 0$ imposed in the course of calculation, form factors are known only at space-like momentum transfer $q^2 = -q_\perp^2 \leq 0$. On the other hand, only time-like form factors are relevant in physical decay processes. Namely, in the exclusive non-leptonic decays, the form factor at maximally recoiling ($q^2 \simeq 0$) is required; while the q^2 -dependent behavior in the full $q^2 > 0$ region is needed in semileptonic \bar{B}_s decays. In order to have the behavior in the whole q^2 region, we adopt the parametrization

$$F(q^2) = \frac{F(0)}{1 - aq^2/m_{B_s}^2 + b(q^2/m_{B_s}^2)^2}, \quad (36)$$

where F denotes any generic form factors V, A_0, A_1, A_2 for $B_s \rightarrow D_s^*$, or A, V_0, V_1, V_2 for $B_s \rightarrow D_{s1}$. These parameters (F, a, b) will be fitted in the space-like region ($-20\text{GeV}^2 < q^2 < 0$). Then, the form factors will be extrapolated to the time-like region.

With the above input parameters, our results for the form factors are collected in table I, where the uncertainties are from the shape parameters of the LFWFs and the constituent quark masses. Our strategy for the uncertainties is as follows. With the central value for quark masses, we first fix shape parameters so that these values can reproduce the adopted decay constants. Secondly, we will also compute the errors caused by quark masses but keeping the shape parameters unchanged. The final uncertainties for the form factors and physical observables will be added in quadrature. We plot the q^2 -dependence of the form factors in Fig. 2~6 for $B_s \rightarrow D_s^*, D_{s1}({}^3P_1), D_{s1}({}^1P_1), D_{s1}(P_1^{1/2})$, and $D_{s1}(P_1^{3/2})$, respectively.

Several remarks are given in order. Firstly, the $B_s \rightarrow D_s^*$ form factors are related to the $B \rightarrow D^*$ form factors by the flavor SU(3) symmetry. Compared with the computation in Ref. [28]

$$\begin{aligned} V^{BD^*}(q^2) &= \frac{0.75}{1 - 1.29q^2/m_B^2 + 0.45(q^2/m_B^2)^2}, & A_0^{BD^*}(q^2) &= \frac{0.64}{1 - 1.30q^2/m_B^2 + 0.31(q^2/m_B^2)^2}, \\ A_1^{BD^*}(q^2) &= \frac{0.63}{1 - 0.65q^2/m_B^2 + 0.02(q^2/m_B^2)^2}, & A_2^{BD^*}(q^2) &= \frac{0.61}{1 - 1.14q^2/m_B^2 + 0.52(q^2/m_B^2)^2}, \end{aligned} \quad (37)$$

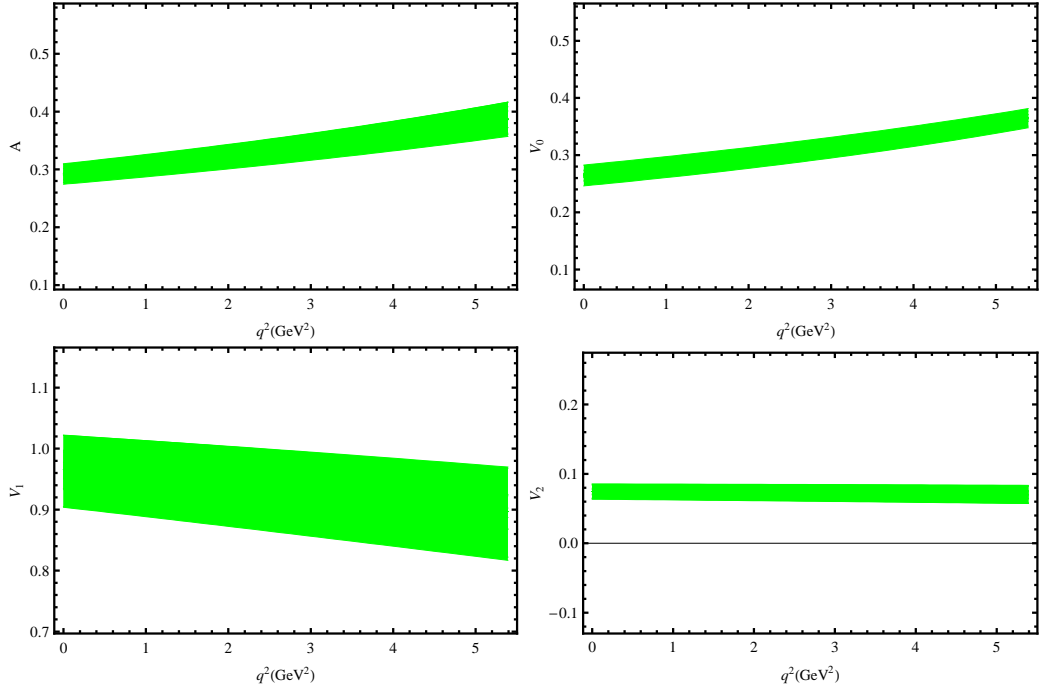


FIG. 3: The q^2 -dependence of the $B_s \rightarrow D_s(3040)$ form factors with $^{2S+1}L_J = ^3P_1$

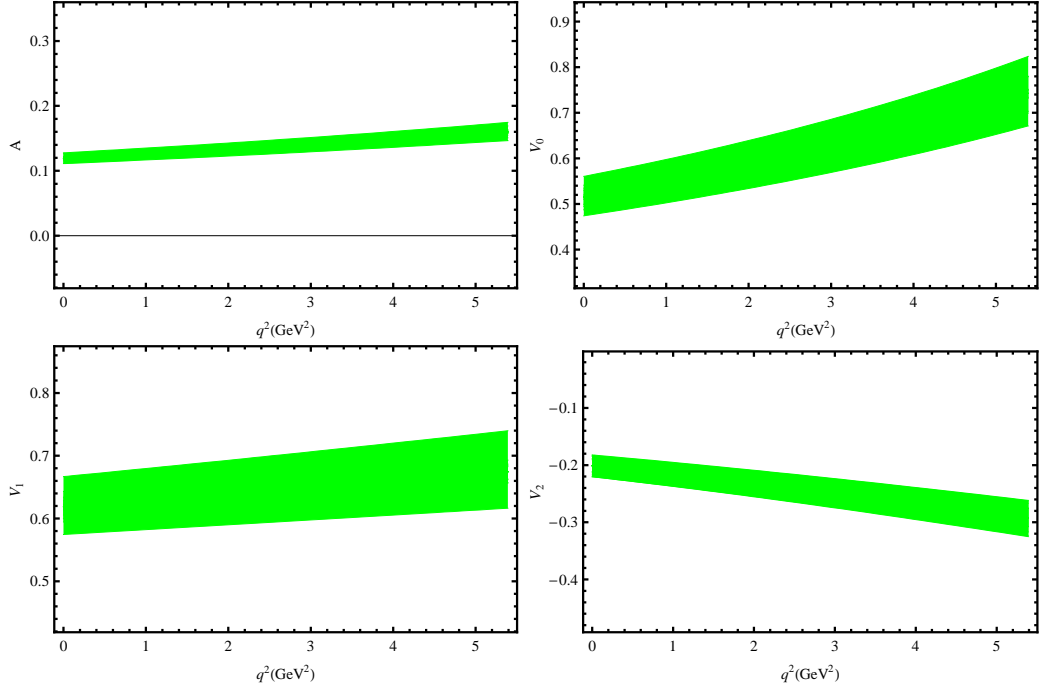


FIG. 4: The q^2 -dependence of the $B_s \rightarrow D_{s1}(3040)$ form factors with $^{2S+1}L_J = ^1P_1$

we can see that our predictions are compatible with their results. The small differences originate from the SU(3) symmetry breaking effects in the constituent quark, hadron masses, and decay constants of the initial and final mesons.

From the results in table I, we can see that although most $B_s \rightarrow D_{s1}$ form factors are smaller than the relevant $B_s \rightarrow D_s^*$ ones, they are still large enough. It implies that the $B_s \rightarrow D_{s1}$ decay channels are very likely to be observable. In particular, the large form factors $V_1^{B_s D_{s1}(P_1^{3/2})}$ and $V_1^{B_s D_{s1}(^1P_1)}$ directly predict the sizable production

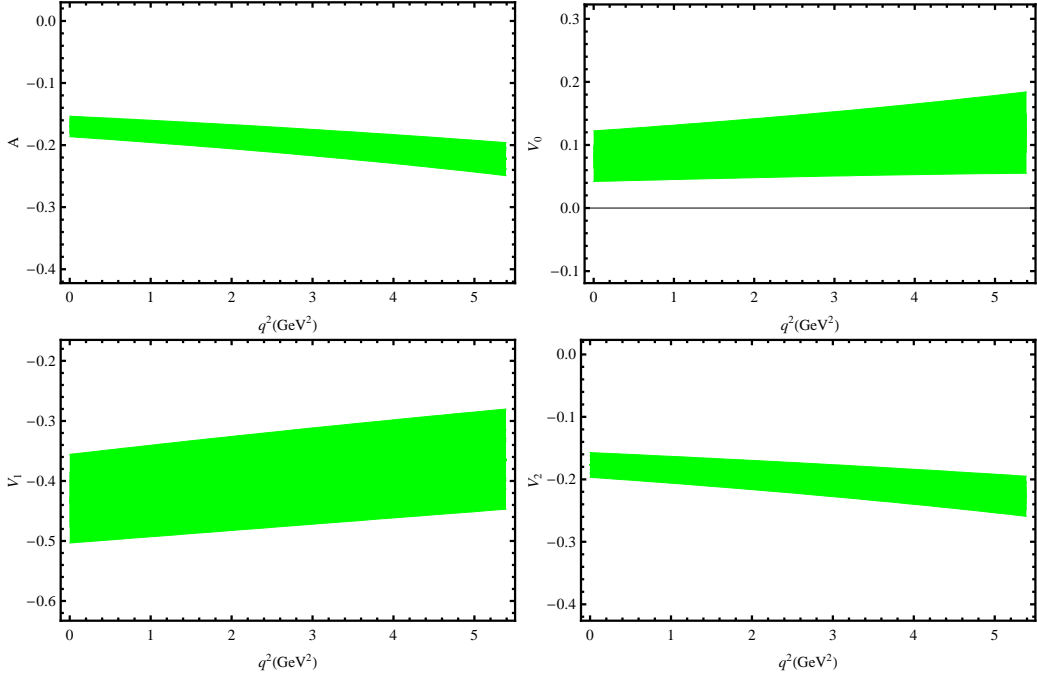


FIG. 5: The q^2 -dependence of the $B_s \rightarrow D_s(3040)$ form factors with the quantum numbers $P_1^{1/2}$

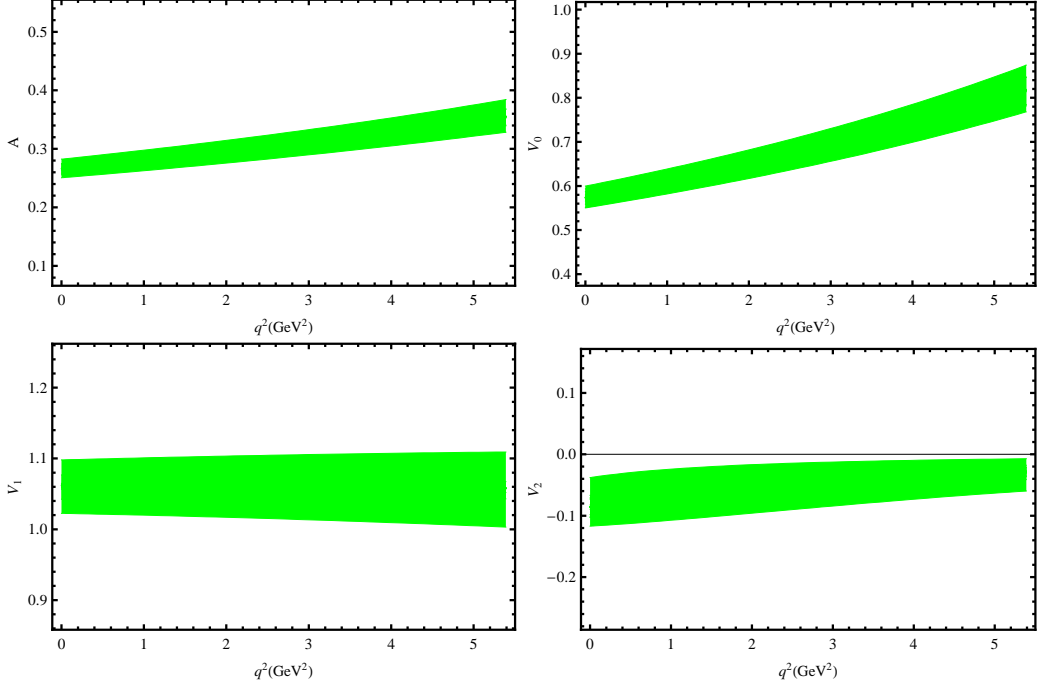


FIG. 6: The q^2 -dependence of the $B_s \rightarrow D_s(3040)$ form factors with the quantum numbers $P_1^{3/2}$

rates in nonleptonic B_s decays, which will be shown in the following section.

One important feature of the $B_s \rightarrow D_s^*$ form factors is that they become larger with the increasing q^2 . However, not all the $B_s \rightarrow D_{s1}$ form factors have this universal behavior. For instance, the form factor $V_1^{B_s D_{s1}({}^3P_1)}$ decreases with the increasing q^2 .

Most form factors have the uncertainties of the order 10% but some of them can reach 20%. The uncertainties are denoted by the bands in Figs.(3-6). The q^2 -dependent parameters of $V_2^{B_s D_s(A^{3/2})}$ also suffer from large uncertainties.

TABLE I: $B_s \rightarrow D_s^*$ and $B_s \rightarrow D_s(3040)$ form factors. Four sets of results are shown for $D_s(3040)$, with different assignments of quantum numbers.

	$F_i(q^2 = 0)$	$F_i(q_{\text{max}}^2)$	a_i	b_i
$V^{B_s D_s^*}$	$0.74^{+0.05}_{-0.05}$	$1.27^{+0.13}_{-0.12}$	$1.34^{+0.11}_{-0.10}$	$0.57^{+0.15}_{-0.13}$
$A_0^{B_s D_s^*}$	$0.63^{+0.04}_{-0.04}$	$1.05^{+0.06}_{-0.06}$	$1.30^{+0.09}_{-0.09}$	$0.54^{+0.14}_{-0.12}$
$A_1^{B_s D_s^*}$	$0.61^{+0.03}_{-0.03}$	$0.82^{+0.05}_{-0.05}$	$0.71^{+0.09}_{-0.08}$	$0.08^{+0.05}_{-0.04}$
$A_2^{B_s D_s^*}$	$0.59^{+0.04}_{-0.04}$	$0.97^{+0.09}_{-0.08}$	$1.24^{+0.10}_{-0.09}$	$0.48^{+0.13}_{-0.11}$
$A^{B_s D_{s1}({}^3P_1)}$	$0.29^{+0.03}_{-0.03}$	$0.39^{+0.05}_{-0.05}$	$1.36^{+0.12}_{-0.12}$	$0.26^{+0.06}_{-0.04}$
$V_0^{B_s D_{s1}({}^3P_1)}$	$0.27^{+0.02}_{-0.02}$	$0.37^{+0.02}_{-0.02}$	$1.52^{+0.10}_{-0.10}$	$0.30^{+0.06}_{-0.05}$
$V_1^{B_s D_{s1}({}^3P_1)}$	$0.97^{+0.09}_{-0.10}$	$0.90^{+0.11}_{-0.12}$	$-0.35^{+0.15}_{-0.18}$	$0.33^{+0.14}_{-0.11}$
$V_2^{B_s D_{s1}({}^3P_1)}$	$0.07^{+0.02}_{-0.02}$	$0.07^{+0.02}_{-0.02}$	$-0.25^{+0.39}_{-0.46}$	$0.53^{+0.31}_{-0.23}$
$A^{B_s D_{s1}({}^1P_1)}$	$0.12^{+0.01}_{-0.01}$	$0.16^{+0.02}_{-0.02}$	$1.50^{+0.10}_{-0.10}$	$0.71^{+0.17}_{-0.14}$
$V_0^{B_s D_{s1}({}^1P_1)}$	$0.52^{+0.06}_{-0.06}$	$0.74^{+0.10}_{-0.09}$	$1.73^{+0.11}_{-0.11}$	$0.48^{+0.09}_{-0.08}$
$V_1^{B_s D_{s1}({}^1P_1)}$	$0.62^{+0.06}_{-0.06}$	$0.68^{+0.07}_{-0.07}$	$0.46^{+0.12}_{-0.12}$	$0.12^{+0.04}_{-0.03}$
$V_2^{B_s D_{s1}({}^1P_1)}$	$-0.20^{+0.03}_{-0.04}$	$-0.29^{+0.06}_{-0.06}$	$2.03^{+0.12}_{-0.12}$	$1.94^{+0.32}_{-0.26}$
$A^{B_s D_{s1}(P_1^{1/2})}$	$-0.17^{+0.03}_{-0.02}$	$-0.22^{+0.04}_{-0.04}$	$1.29^{+0.14}_{-0.15}$	$0.14^{+0.06}_{-0.03}$
$V_0^{B_s D_{s1}(P_1^{1/2})}$	$0.08^{+0.05}_{-0.05}$	$0.12^{+0.08}_{-0.09}$	$2.15^{+0.08}_{-0.25}$	$1.8^{+3.7}_{-1.0}$
$V_1^{B_s D_{s1}(P_1^{1/2})}$	$-0.43^{+0.11}_{-0.10}$	$-0.37^{+0.11}_{-0.11}$	$-0.87^{+0.32}_{-0.43}$	$0.67^{+0.38}_{-0.26}$
$V_2^{B_s D_{s1}(P_1^{1/2})}$	$-0.18^{+0.03}_{-0.03}$	$-0.23^{+0.05}_{-0.05}$	$1.21^{+0.16}_{-0.19}$	$0.21^{+0.07}_{-0.04}$
$A^{B_s D_{s1}(P_1^{3/2})}$	$0.27^{+0.02}_{-0.02}$	$0.36^{+0.03}_{-0.03}$	$1.41^{+0.10}_{-0.10}$	$0.40^{+0.08}_{-0.06}$
$V_0^{B_s D_{s1}(P_1^{3/2})}$	$0.57^{+0.04}_{-0.04}$	$0.82^{+0.07}_{-0.07}$	$1.67^{+0.11}_{-0.11}$	$0.42^{+0.08}_{-0.07}$
$V_1^{B_s D_{s1}(P_1^{3/2})}$	$1.06^{+0.04}_{-0.04}$	$1.06^{+0.05}_{-0.06}$	$0.01^{+0.07}_{-0.08}$	$0.17^{+0.05}_{-0.04}$
$V_2^{B_s D_{s1}(P_1^{3/2})}$	$-0.09^{+0.06}_{-0.04}$	$-0.03^{+0.03}_{-0.04}$	-6^{+5}_{-10}	25^{+17}_{-10}

It is fortunate that the magnitude of this form factor is small. Thus, it has little influence on physical processes.

IV. APPLICATIONS TO B_s DECAYS

In this section, we will use the above determined form factors to predict semileptonic $B_s \rightarrow D_s^*(D_s(3040))\ell\bar{\nu}$ and nonleptonic B_s decays. For nonleptonic B_s decays, the factorization assumption will be used to decompose the decay amplitudes into the form factors and the decay constant of the emitted meson. In particular, we will only consider the color-allowed decay channels where factorization assumptions work well and the nonfactorizable contributions are typically small.

A. Semileptonic B_s decays

With the form factors available, we can investigate the semileptonic $B_s \rightarrow D_s^*$ and $B_s \rightarrow D_s(3040)$ decays

$$\begin{aligned}
 \frac{d\Gamma^M}{dq^2} &= \sum_{i=L,\pm} \frac{d\Gamma_i^M}{dq^2}, \\
 \frac{d\Gamma_{L,\pm}^M}{dq^2} &= \frac{|G_F V_{cb}|^2 \sqrt{\lambda_M}}{256 m_{B_s}^3 \pi^3 q^2} \left(1 - \frac{m_\ell^2}{q^2}\right)^2 (X_L^M, X_\pm^M)
 \end{aligned} \tag{38}$$

where M denotes D_s^* or $D_s(3040)$, $\lambda_M = \lambda(m_{B_s}^2, m_M^2, q^2)$, and $\lambda(a^2, b^2, c^2) = (a^2 - b^2 - c^2)^2 - 4b^2c^2$. The subscript (L, \pm) denotes the three polarizations of the vector and axial-vector $\bar{c}s$ meson along its momentum direction $(0, \pm 1)$. In terms of the angular distributions, we can study the forward-backward asymmetries (FBAs) of lepton which are

defined as

$$\frac{dA_{FB}^M}{dq^2} = \frac{\int_0^1 dz(d\Gamma^M/dq^2 dz) - \int_{-1}^0 dz(d\Gamma^M/dq^2 dz)}{\int_0^1 dz(d\Gamma^M/dq^2 dz) + \int_{-1}^0 dz(d\Gamma^M/dq^2 dz)}$$

where $z \equiv \cos \theta$ and the angle θ is the polar angle of the lepton with respect to the moving direction of $D_s^*(D_{s1})$ in the lepton pair rest frame. Explicitly, we have

$$\begin{aligned} \frac{dA_{FB}^{D_s^*}}{dq^2} &= \frac{1}{X_L^{D_s^*} + X_+^{D_s^*} + X_-^{D_s^*}} \left(2m_\ell^2 \sqrt{\lambda_{D_s^*}} h_0^{D_s^*}(q^2) A_0(q^2) - 4q^4 \sqrt{\lambda_{D_s^*}} A_1(q^2) V(q^2) \right), \\ \frac{dA_{FB}^{D_{s1}}}{dq^2} &= \frac{1}{X_L^{D_{s1}} + X_+^{D_{s1}} + X_-^{D_{s1}}} \left(2m_\ell^2 \sqrt{\lambda_{D_{s1}}} h_0^{D_{s1}}(q^2) V_0(q^2) - 4q^4 \sqrt{\lambda_{D_{s1}}} V_1(q^2) A(q^2) \right), \end{aligned} \quad (39)$$

where

$$\begin{aligned} X_L^{D_s^*} &= \frac{2}{3} \left[(2q^2 + m_\ell^2)(h_0^{D_s^*}(q^2))^2 + 3\lambda_{D_s^*} m_\ell^2 A_0^2(q^2) \right], \\ X_\pm^{D_s^*} &= \frac{2q^2}{3} (2q^2 + m_\ell^2) \left[(m_{B_s} + m_{D_s^*}) A_1(q^2) \mp \frac{\sqrt{\lambda_{D_s^*}}}{m_{B_s} + m_{D_s^*}} V(q^2) \right]^2, \\ h_0^{D_s^*}(q^2) &= \frac{1}{2m_{D_s^*}} \left[(m_{B_s}^2 - m_{D_s^*}^2 - q^2)(m_{B_s} + m_{D_s^*}) A_1(q^2) - \frac{\lambda_{D_s^*}}{m_{B_s} + m_{D_s^*}} A_2(q^2) \right], \\ X_L^{D_{s1}} &= \frac{2}{3} \left[(2q^2 + m_\ell^2)(h_0^{D_{s1}}(q^2))^2 + 3\lambda_{D_{s1}} m_\ell^2 V_0^2(q^2) \right], \\ X_\pm^{D_{s1}} &= \frac{2q^2}{3} (2q^2 + m_\ell^2) \left[(m_{B_s} - m_{D_{s1}}) V_1(q^2) \mp \frac{\sqrt{\lambda_{D_{s1}}}}{m_{B_s} - m_{D_{s1}}} A(q^2) \right]^2, \\ h_0^{D_{s1}}(q^2) &= \frac{1}{2m_{D_{s1}}} \left[(m_{B_s}^2 - m_{D_{s1}}^2 - q^2)(m_{B_s} - m_{D_{s1}}) V_1(q^2) - \frac{\lambda_{D_{s1}}}{m_{B_s} - m_{D_{s1}}} V_2(q^2) \right]. \end{aligned} \quad (40)$$

Integrating over the q^2 , we obtain the partial decay width and integrated angular asymmetry for the $B_s \rightarrow D_{sJ}$ decay modes:

$$\Gamma^M = \Gamma_L^M + \Gamma_+^M + \Gamma_-^M, \quad A_{FB}^M = \frac{1}{\Gamma^M} \int dq^2 \int_{-1}^1 \text{sign}(z) dz (d\Gamma^M/dq^2 dz)$$

with

$$\Gamma_{L,\pm}^M = \int_{m_i^2}^{(m_{B_s} - m_M)^2} dq^2 \frac{d\Gamma_{L,\pm}^M}{dq^2}. \quad (41)$$

Since there are three different polarizations, it is also meaningful to define the polarization fraction

$$f_L = \frac{\Gamma_L}{\Gamma_L + \Gamma_+ + \Gamma_-}. \quad (42)$$

Our results for the branching fractions, FBAs and polarizations are given in Table II, where $V_{cb} = 0.0412$ is employed [39]. The uncertainties are from the form factors. Several remarks are given in order. Our result for the $\mathcal{B}(B_s \rightarrow D_s^* l \bar{\nu})$ is well consistent with the QCD sum rules in Ref. [51], $\mathcal{B}(B_s \rightarrow D_s^* l \bar{\nu}) = (5.6 \pm 0.2)\%$, but is smaller than the prediction in Ref. [52] by roughly 40%, $\mathcal{B}(B_s \rightarrow D_s^* e \bar{\nu}) = (7.09 \pm 0.88)\%$. At present there are no experimental data on the semileptonic B_s decays into D_s^* . Interestingly, our predictions are close to the $B \rightarrow D^* l \bar{\nu}$ data [39] which can be related to the B_s decays by the flavor SU(3) symmetry

$$\mathcal{B}(\bar{B}^0 \rightarrow D^{*+} l^- \bar{\nu}) = (5.16 \pm 0.11)\%, \quad \mathcal{B}(\bar{B}^0 \rightarrow D^{*+} \tau^- \bar{\nu}_\tau) = (1.6 \pm 0.5)\%. \quad (43)$$

Since the flavor symmetry breaking is at a few percent level, our results are also supported by the nonleptonic B and B_s decay data [39]

$$\mathcal{B}(\bar{B}^0 \rightarrow D^+ \pi^-) = (2.68 \pm 0.23) \times 10^{-3} \sim \mathcal{B}(\bar{B}_s^0 \rightarrow D_s^+ \pi^-) = (3.2 \pm 0.9) \times 10^{-3}. \quad (44)$$

TABLE II: Branching ratios, polarization fractions and angular asymmetries for $B_s \rightarrow D_s^*$ and $B_s \rightarrow D_s(3040)$

	$\ell = \mu$	$\ell = \tau$
$\mathcal{B}(\bar{B}_s^0 \rightarrow D_s^{*+} \ell \bar{\nu}_\ell)$	$(5.2^{+0.6}_{-0.6}) \times 10^{-2}$	$(1.3^{+0.2}_{-0.1}) \times 10^{-2}$
$f_L(\bar{B}_s^0 \rightarrow D_s^{*+} \ell \bar{\nu}_\ell)$	$(51.3^{+1.2}_{-1.3}) \times 10^{-2}$	$(44.5^{+0.8}_{-0.9}) \times 10^{-2}$
$A_{\text{FB}}(\bar{B}_s^0 \rightarrow D_s^{*+} \ell \bar{\nu}_\ell)$	$(-21.7^{+1.4}_{-1.5}) \times 10^{-2}$	$(-5.6^{+1.4}_{-1.5}) \times 10^{-2}$
$\mathcal{B}(\bar{B}_s^0 \rightarrow D_{s1}^+(^3P_1) \ell \bar{\nu}_\ell)$	$(2.3^{+0.3}_{-0.3}) \times 10^{-3}$	$(6.1^{+1.2}_{-1.2}) \times 10^{-5}$
$f_L(\bar{B}_s^0 \rightarrow D_{s1}^+(^3P_1) \ell \bar{\nu}_\ell)$	$(43.3^{+3.9}_{-4.2}) \times 10^{-2}$	$(36.0^{+1.9}_{-2.2}) \times 10^{-2}$
$A_{\text{FB}}(\bar{B}_s^0 \rightarrow D_{s1}^+(^3P_1) \ell \bar{\nu}_\ell)$	$(-39.7^{+4.2}_{-4.0}) \times 10^{-2}$	$(-16.6^{+4.0}_{-4.2}) \times 10^{-2}$
$\mathcal{B}(\bar{B}_s^0 \rightarrow D_{s1}^+(^1P_1) \ell \bar{\nu}_\ell)$	$(2.9^{+0.6}_{-0.6}) \times 10^{-3}$	$(5.2^{+1.2}_{-1.0}) \times 10^{-5}$
$f_L(\bar{B}_s^0 \rightarrow D_{s1}^+(^1P_1) \ell \bar{\nu}_\ell)$	$(84.0^{+2.2}_{-2.3}) \times 10^{-2}$	$(65.9^{+3.1}_{-3.0}) \times 10^{-2}$
$A_{\text{FB}}(\bar{B}_s^0 \rightarrow D_{s1}^+(^1P_1) \ell \bar{\nu}_\ell)$	$(-6.8^{+1.4}_{-1.5}) \times 10^{-2}$	$(19.0^{+2.5}_{-2.6}) \times 10^{-2}$
$\mathcal{B}(\bar{B}_s^0 \rightarrow D_{s1}^+(P_1^{1/2}) \ell \bar{\nu}_\ell)$	$(3.5^{+1.1}_{-1.0}) \times 10^{-4}$	$(9.9^{+4.4}_{-3.5}) \times 10^{-6}$
$f_L(\bar{B}_s^0 \rightarrow D_{s1}^+(P_1^{1/2}) \ell \bar{\nu}_\ell)$	$(9.8^{+11.9}_{-3.4}) \times 10^{-2}$	$(18.0^{+2.3}_{-0.2}) \times 10^{-2}$
$A_{\text{FB}}(\bar{B}_s^0 \rightarrow D_{s1}^+(P_1^{1/2}) \ell \bar{\nu}_\ell)$	$(-65.0^{+13.4}_{-3.2}) \times 10^{-2}$	$(-47.6^{+8.6}_{-2.3}) \times 10^{-2}$
$\mathcal{B}(\bar{B}_s^0 \rightarrow D_{s1}^+(P_1^{3/2}) \ell \bar{\nu}_\ell)$	$(4.0^{+0.4}_{-0.5}) \times 10^{-3}$	$(9.7^{+0.8}_{-0.8}) \times 10^{-5}$
$f_L(\bar{B}_s^0 \rightarrow D_{s1}^+(P_1^{3/2}) \ell \bar{\nu}_\ell)$	$(63.9^{+3.5}_{-4.0}) \times 10^{-2}$	$(49.9^{+1.8}_{-1.6}) \times 10^{-2}$
$A_{\text{FB}}(\bar{B}_s^0 \rightarrow D_{s1}^+(P_1^{3/2}) \ell \bar{\nu}_\ell)$	$(-22.2^{+1.9}_{-2.1}) \times 10^{-2}$	$(2.0^{+0.7}_{-0.5}) \times 10^{-2}$

Furthermore our results show that the polarization fractions and angular asymmetries are sizable and can be tested at the hadron collider and the Super B experiment in the near future.

Compared with $B_s \rightarrow D_s^* l \bar{\nu}$, the BRs of the $B_s \rightarrow D_s(3040) l \bar{\nu}$ ($l = \mu$) decays are typically smaller by one order of magnitude. However, if $D_s(3040)$ has the quantum number $P_1^{1/2}$, the BR would be suppressed by two orders of magnitude as a consequence of the tiny form factors. The mass of the $D_s(3040)$ is larger than that of D_s^* , making the phase space in $B_s \rightarrow D_{s1} \tau \bar{\nu}_\tau$ much smaller and inducing further suppressions of the BRs. Nevertheless, the BRs are still large enough to measure in the future. For example, the LHCb experiment will produce more than 10^6 B_s mesons per running year, implying that a plenty of the $D_s(3040)$ events will be generated.

Although the production rates for $D_s(3040)$ under the two different descriptions 3P_1 and 1P_1 are similar, their polarizations are quite different. For the 3P_1 assignment, the form factor V_1 is much larger than the other ones. The interference between different form factors does not manifest. Since both longitudinal and transverse polarizations depend on this large V_1 , the polarization fraction is close to 50%. For 1P_1 , the magnitude of V_2 is enhanced and it has a different sign with V_1 . These two form factors will provide constructive contributions to the longitudinal polarization as shown in Eq. (40), and lead to a larger value for f_L .

The angular asymmetries in $B_s \rightarrow D_{s1} l \bar{\nu}$ with $D_{s1} = (^3P_1, ^1P_1)$ are also different. If the lepton is a light muon, the mass terms in the angular asymmetries as in Eq. (39) are negligible. Thus, the form factor product $V_1(q^2)A(q^2)$ determines the size of the angular asymmetries. For 3P_1 , the product is much larger than that of the 1P_1 assignment. So is the angular asymmetry, but with a negative sign. If the lepton is changed to a massive tau, the two terms in Eq. (39) give destructive contributions, which will reduce the modulo of the angular asymmetries for 3P_1 and change the sign for the 1P_1 .

The above analysis is also similar for the other assignment basis. One exceptional case is the polarization fraction for the $P_1^{1/2}$. All form factors are relatively small, and the cancelation between V_1 and V_2 in the longitudinal polarization results in a small polarization fraction f_L .

B. Nonleptonic B_s decays

After the contraction of the highly-virtual degrees of freedom such as the W, Z bosons, the effective Hamiltonian governing nonleptonic $B_s \rightarrow D_{sJ}$ decays is given as

$$H_{\text{eff}} = \frac{G_F}{\sqrt{2}} \sum_{p,D} V_{cb} V_{pD}^* (C_1 O_1 + C_2 O_2) + h.c., \quad (45)$$

with the four quark operators

$$O_1 = [\bar{c}^\alpha \gamma^\mu (1 - \gamma_5) b^\alpha] [\bar{D}^\beta \gamma_\mu (1 - \gamma_5) p^\beta], \quad O_2 = [\bar{c}^\alpha \gamma^\mu (1 - \gamma_5) b^\beta] [\bar{D}^\beta \gamma_\mu (1 - \gamma_5) p^\alpha], \quad (46)$$

and C_1 and C_2 being their Wilson coefficients which arise from the perturbative coefficients over the m_b scale. We use $a_1 = C_1 + C_2/3 = 1.07$ [34]. In the above equation, it is labeled $p = u, c$ and $D = d, s$, while α and β are color indices. The CKM matrix elements are employed as $V_{ud} = 0.97418$, $|V_{cd}| = 0.23$, $V_{cs} = 0.997$ and $V_{us} = 0.2255$ [39].

Nonleptonic $B_s \rightarrow D_{sJ} M$ decays involve one more meson and the two final state mesons will get entangled with each other. In case of the M being a light meson, it is feasible to show that the decay amplitude can be decomposed into two individual parts. This method is known as factorization [46–48]. The light meson moves very fast in the B_s rest frame and it is made of collinear quark fields and gluon fields. On the contrary, the B_s meson and the recoiled D_{sJ} are almost at rest and the dynamic degree of freedom is the heavy quark, the light antiquark with quantum fluctuations. The complete set of the degrees of freedom in these heavy mesons has typically small momentum¹ and is characterized by the soft fields. Interactions between the two different sectors are forbidden at the leading power and these two sectors are dynamically separated. The elegant proof rooted in the quantum field theory has been given in Ref. [49], where an effective field theory built in Ref. [50] has been used.

Under such an effective theory, the matrix element of the four-quark operators in two-body B_s decays is expressed in terms of the $B_s \rightarrow D_{sJ}$ form factors, which have been computed in the above, together with the convolution of a hard kernel $T(u)$ and the light-cone distribution amplitude $\phi(u)$ of the light meson. The hard kernel can be computed in the expansion of α_s , and particularly at the leading order $T(u) = 1 + \mathcal{O}(\alpha_s)$. In this case, the analysis based on the effective theory recovers the naive factorization in which the decay amplitudes for $\overline{B}_s \rightarrow D_s^{*+} \pi^-$ and $\overline{B}_s \rightarrow D_s^{*+} \rho^-$ are given as

$$\begin{aligned} \mathcal{A}(\overline{B}_s^0 \rightarrow D_s^{*+} \pi^-) &= \frac{G_F}{\sqrt{2}} V_{cb} V_{ud}^* a_1 f_\pi A_0(m_\pi^2) \sqrt{\lambda(m_{B_s}^2, m_{D_s^*}^2, m_\pi^2)}, \\ \mathcal{A}_L(\overline{B}_s^0 \rightarrow D_s^{*+} \rho^-) &= \frac{-iG_F}{\sqrt{2}} V_{cb} V_{ud}^* a_1 f_\rho h_0^{D_s^*}(m_\rho^2), \\ \mathcal{A}_N(\overline{B}_s^0 \rightarrow D_s^{*+} \rho^-) &= \frac{-iG_F}{\sqrt{2}} V_{cb} V_{ud}^* a_1 f_\rho (m_{B_s} + m_{D_s^*}) m_\rho A_1(m_\rho^2), \\ \mathcal{A}_T(\overline{B}_s^0 \rightarrow D_s^{*+} \rho^-) &= \frac{-iG_F}{\sqrt{2}} V_{cb} V_{ud}^* a_1 f_\rho \frac{\sqrt{\lambda(m_{B_s}^2, m_{D_s^*}^2, m_\rho^2)}}{(m_{B_s} + m_{D_s^*})} m_\rho V(m_\rho^2). \end{aligned} \quad (47)$$

In the above, the amplitude of $\overline{B}_s \rightarrow D_s^{*+} (P_{D_s^*}) \rho^- (P_\rho)$ has been decomposed according to the Lorentz structures

$$\mathcal{A} = \mathcal{A}_L + \epsilon_{D_s^*}^*(T) \cdot \epsilon_\rho^*(T) \mathcal{A}_N + i \mathcal{A}_T \epsilon_{\alpha\beta\gamma\rho} \epsilon_{D_s^*}^{*\alpha} \epsilon_\rho^{*\beta} \frac{2P_{D_s^*}^\gamma P_\rho^\rho}{\sqrt{\lambda(m_{B_s}^2, m_{D_s^*}^2, m_\rho^2)}}. \quad (48)$$

We will also consider the decay channels in which the light meson (π^-, ρ^-) is replaced by K^-, D^-, D_s^- or K^{*-}, D^{*-}, D_s^{*-} . The partial decay width of $\overline{B}_s \rightarrow D_s^* P$, where P denotes a pseudoscalar meson, is given by

$$\Gamma(\overline{B}_s \rightarrow D_s^* P) = \frac{|\vec{p}|}{8\pi m_{B_s}^2} |\mathcal{A}(\overline{B}_s \rightarrow D_s^* P)|^2, \quad (49)$$

with $|\vec{p}|$ being the three-momentum of the D_s^* in the B_s meson rest frame. For $\overline{B}_s \rightarrow D_s^* V$, the partial decay width is the summation of the three polarizations

$$\Gamma(\overline{B}_s \rightarrow D_s^* V) = \frac{|\vec{p}|}{8\pi m_{B_s}^2} \left(|\mathcal{A}_0(\overline{B}_s \rightarrow D_s^* V)|^2 + 2 |\mathcal{A}_N(\overline{B}_s \rightarrow D_s^* V)|^2 + 2 |\mathcal{A}_T(\overline{B}_s \rightarrow D_s^* V)|^2 \right). \quad (50)$$

In the decay amplitudes for the channels involving D_{s1} , the form factors are replaced correspondingly and $m_{B_s} + m_{D_s^*}$ is replaced by $m_{B_s} - m_{D_{s1}}$.

Before proceeding, it is worth mentioning that the proof of factorization of B_s decays into two charmed mesons such as $B_s \rightarrow D_s^* D_s^*$ is absent in the literature. Nevertheless, since only the color-allowed tree diagrams are considered in this work, the nonfactorizable diagrams are typically small and the factorization usually works very well [46–48]. For instance, our predictions of the branching fractions of these channels are well consistent with the experimental results. This verifies the applicability of the factorization approach.

¹ For the heavy quark, it means the residual momentum after separating the large label momentum.

TABLE III: Branching ratios of nonleptonic B_s decays into D_s^* and a comparison with theoretical results[53–55] and experimental data

	Factorization [53]	perturbative QCD [54, 55]	This work	Exp.
$\bar{B}_s^0 \rightarrow D_s^{*+} \pi^-$	2.8×10^{-3}	$(2.42^{+1.37}_{-1.06}) \times 10^{-3}$	$(3.5^{+0.4}_{-0.4}) \times 10^{-3}$	$(2.4^{+0.7}_{-0.6}) \times 10^{-3}$
$\bar{B}_s^0 \rightarrow D_s^{*+} K^-$	2.1×10^{-4}	$(1.65^{+1.06}_{-0.82}) \times 10^{-4}$	$(2.8^{+0.3}_{-0.3}) \times 10^{-4}$	
$\bar{B}_s^0 \rightarrow D_s^{*+} D^-$	3.3×10^{-4}	$(2.7^{+1.9}_{-1.4}) \times 10^{-4}$	$(3.7^{+0.4}_{-0.4}) \times 10^{-4}$	
$\bar{B}_s^0 \rightarrow D_s^{*+} D_s^-$	7.4×10^{-3}	$(7.0^{+4.8}_{-3.8}) \times 10^{-3}$	$(9.2^{+1.1}_{-1.1}) \times 10^{-3}$	
$\bar{B}_s^0 \rightarrow D_s^{*+} \rho^-$	8.9×10^{-3}	$(5.69^{+3.59}_{-2.84}) \times 10^{-3}$	$(11.8^{+3.3}_{-3.1}) \times 10^{-3}$	$(11.3^{+1.4}_{-1.3}) \times 10^{-3}$
$\bar{B}_s^0 \rightarrow D_s^{*+} K^{*-}$	4.8×10^{-4}	$(3.47^{+2.24}_{-1.72}) \times 10^{-4}$	$(5.5^{+0.6}_{-0.6}) \times 10^{-4}$	
$\bar{B}_s^0 \rightarrow D_s^{*+} D^{*-}$	1.0×10^{-3}	$(3.9^{+2.9}_{-2.3}) \times 10^{-4}$	$(8.6^{+1.0}_{-0.9}) \times 10^{-4}$	
$\bar{B}_s^0 \rightarrow D_s^{*+} D_s^{*-}$	2.9×10^{-2}	$(9.9^{+7.7}_{-6.2}) \times 10^{-3}$	$(23.6^{+4.0}_{-3.8}) \times 10^{-3}$	$(3.1^{+1.4}_{-1.3})\%$

TABLE IV: Branching ratios of nonleptonic B_s decays into $D_s(3040)$ with different assignments

	π^-	K^-	D^-	D_s^-
$\bar{B}_s^0 \rightarrow D_{s1}^+(^3P_1)$	$(3.2^{+0.5}_{-0.5}) \times 10^{-4}$	$(2.5^{+0.4}_{-0.4}) \times 10^{-5}$	$(1.4^{+0.2}_{-0.2}) \times 10^{-5}$	$(2.8^{+0.4}_{-0.4}) \times 10^{-4}$
$\bar{B}_s^0 \rightarrow D_{s1}^+(^1P_1)$	$(1.2^{+0.3}_{-0.3}) \times 10^{-3}$	$(9.3^{+2.2}_{-2.0}) \times 10^{-5}$	$(5.7^{+1.5}_{-1.3}) \times 10^{-5}$	$(1.1^{+0.3}_{-0.3}) \times 10^{-3}$
$\bar{B}_s^0 \rightarrow D_{s1}^+(P_1^{1/2})$	$(3.0^{+4.5}_{-2.9}) \times 10^{-5}$	$(2.3^{+3.5}_{-2.3}) \times 10^{-6}$	$(1.5^{+2.2}_{-1.5}) \times 10^{-6}$	$(3.0^{+4.4}_{-3.1}) \times 10^{-5}$
$\bar{B}_s^0 \rightarrow D_{s1}^+(P_1^{3/2})$	$(1.5^{+0.2}_{-0.2}) \times 10^{-3}$	$(1.2^{+0.2}_{-0.1}) \times 10^{-4}$	$(6.9^{+1.1}_{-1.0}) \times 10^{-5}$	$(1.4^{+0.2}_{-0.2}) \times 10^{-3}$
	ρ^-	K^{*-}	D^{*-}	D_s^{*-}
$\bar{B}_s^0 \rightarrow D_{s1}^+(^3P_1)$	$(1.3^{+0.2}_{-0.2}) \times 10^{-3}$	$(6.4^{+0.7}_{-0.8}) \times 10^{-5}$	$(6.6^{+1.2}_{-1.2}) \times 10^{-5}$	$(1.4^{+0.3}_{-0.3}) \times 10^{-3}$
$\bar{B}_s^0 \rightarrow D_{s1}^+(^1P_1)$	$(3.0^{+0.7}_{-0.6}) \times 10^{-3}$	$(1.4^{+0.3}_{-0.3}) \times 10^{-4}$	$(4.5^{+0.9}_{-0.8}) \times 10^{-5}$	$(9.0^{+2.0}_{-1.8}) \times 10^{-4}$
$\bar{B}_s^0 \rightarrow D_{s1}^+(P_1^{1/2})$	$(1.6^{+1.0}_{-0.7}) \times 10^{-4}$	$(8.5^{+4.4}_{-3.0}) \times 10^{-6}$	$(1.1^{+0.5}_{-0.4}) \times 10^{-5}$	$(2.4^{+1.1}_{-1.0}) \times 10^{-4}$
$\bar{B}_s^0 \rightarrow D_{s1}^+(P_1^{3/2})$	$(3.3^{+0.6}_{-0.7}) \times 10^{-3}$	$(1.5^{+0.3}_{-0.3}) \times 10^{-4}$	$(8.9^{+0.7}_{-0.7}) \times 10^{-5}$	$(1.9^{+0.2}_{-0.2}) \times 10^{-3}$

Using the above parameters, we directly obtain the branching fractions which are collected in Table III and Table IV. For comparison, we also collect two sets of different theoretical predictions on the $B_s \rightarrow D_s^*$ decays [53–55] and the relevant experimental data [44, 45]. From Table III we can see that our predictions on $B_s \rightarrow D_s^*$ decay channels are consistent with the experimental data within uncertainties. This may also imply that our results for $B_s \rightarrow D_s(3040)$ are reliable. Results in the factorization method [53] are also close to our results but the perturbative QCD predictions [54, 55] are typically smaller. For instance, the central value of the perturbative QCD result of $\bar{B}_s^0 \rightarrow D_s^{*+} D_s^{*-}$ is smaller than our result by a factor of 2.5.

Our uncertainties are from the form factors, i.e., from the quark masses and the shape parameters. Uncertainties in the perturbative QCD approach shown in Table III are from three sets of input parameters: (1) decay constants of $f_{B_s} = (0.24 \pm 0.03)$ GeV (in Ref.[54]) or $f_{B_s} = (0.23 \pm 0.03)$ GeV (in Ref.[55]), and the shape parameters of the B_s wave functions $\omega_b = (0.50 \pm 0.05)$ GeV; (2) the factorization scale (from 0.75t to 1.25t not changing the transverse part) and the hadronic scale $\Lambda_{\text{QCD}} = (0.25 \pm 0.05)$ GeV; (3) the CKM matrix elements V_{cs} and V_{ud} . Among them, the hadronic inputs are found to give the largest uncertainties, while the ones from CKM are the smallest. For instance, the branching fraction of $\bar{B}_s^0 \rightarrow D_s^{*+} \pi^-$ with these three kinds of errors is given as

$$\mathcal{B}(\bar{B}_s^0 \rightarrow D_s^{*+} \pi^-) = (2.42^{+1.12+0.78+0.07}_{-0.72-0.77-0.07}) \times 10^{-3}. \quad (51)$$

Uncertainties in the PQCD approach are larger than our results for several reasons.

- Compared with the f_{B_s} adopted in this work, the uncertainty in their computations is larger by a factor of 2.
- In the PQCD approach, the B_s wave function has such a property that the decay constant can be factorized out and then f_{B_s} is only the normalization constant of the wave functions. In the PQCD approach, the authors have independently estimated these two uncertainties and added them together as their final results. On the contrary, in the covariant LFQM the decay constant can not be factorized, but has been expressed as a convolution form as shown in Eq. (26). In this case, only the decay constant is the origin for the uncertainties, which will be smaller.
- The uncertainties caused by factorization scales and hadronic scales in the PQCD approach characterize higher order QCD corrections and can be viewed as the model-dependent errors (or systematic errors). They are

smaller than but still in similar magnitude with the ones from the B_s wave functions. One particular type of model-dependent uncertainties in this quark model concerns the zero-mode contributions. A direct evaluation of the form factors in the light-front quark model suffers from the non-covariance problem. It is resolved with the inclusion of the zero-mode contributions, i.e. the Z-graph as in the conventional LFQM, and the direct treatment of the spurious terms with the replacement rules as in the covariant LFQM. Different results can be produced. However, at present such computation in the conventional light-front quark model is not available. Therefore, it is not possible to estimate the systematic errors.

In $B_s \rightarrow D_{s1}$ decays with a pseudoscalar meson emitted, the decay amplitudes only involve the form factor V_0 . The large form factors for the $P_1^{3/2}$ and 1P_1 result in large BRs. Similarly, the large uncertainty for $V_0(B_s \rightarrow D_{s1}(P_1^{1/2}))$ also gives large uncertainties to the BRs.

Channels with the emissions of K^- and D^- are suppressed by roughly one order of magnitude compared with the case emitting a pion and D_s meson. This is due to the hierarchy in CKM matrix elements: $|V_{us}| \sim |V_{cd}| \sim 0.22 \ll |V_{ud}| \sim |V_{cs}| \sim 1$.

Under different quantum number assignments for $D_s(3040)$, the branching fractions $B_s \rightarrow D_s(3040)\rho$ and $B_s \rightarrow D_s(3040)D_s^*$ can reach the order of 10^{-3} . But the modes with the emissions of K^* and D^* are smaller by 1 to 2 orders. Nevertheless, all of these channels have a promising prospect on the LHCb experiment with sufficient statistics for the B_s production.

V. CONCLUSIONS

Using the covariant light-front quark model, we have studied the $B_s \rightarrow D_s(3040)$ form factors, including the $B_s \rightarrow D_s^*$ form factors as a byproduct. The form factors are computed in the space-like region and extrapolated to the physical region through a three-parameter form. Those form factors are used to predict the semileptonic and nonleptonic B_s decays. In particular, the predictions on branching fractions, longitudinal polarization fractions and the angular asymmetry, are provided. Our results for $B_s \rightarrow D_s^*$ decays are consistent with the experimental data for the B_s and B decays which are related by the flavor symmetry. For $B_s \rightarrow D_s(3040)$, we find that the branching fractions are large enough to be observed on the LHCb experiment. For instance, the BRs of semileptonic $B_s \rightarrow D_s(3040)l\bar{\nu}$, nonleptonic $B_s \rightarrow D_{s1}\rho$, and $B_s \rightarrow D_{s1}D_s^*$ can reach the order of 10^{-3} . In spite of similar production rates, the different assignments for the $D_s(3040)$ can be distinguished by the polarization fractions and angular asymmetries. We expect more experimental results from the B factories and LHC etc in the near future. They would be helpful to provide deeper insights into the $\bar{c}s$ spectroscopy.

Acknowledgements

This work is supported in part by the National Natural Science Foundation of China under Grant Nos. 10775089, 10805037 and 10947007. W. Wang thanks P. Colangelo for useful discussions and acknowledges Qufu Normal University for the hospitality during his visit. We would like to acknowledge Q. Zhao for carefully reading the manuscript and useful suggestions.

Appendix A: Some specific rules under the p^- integration

When performing the p^- integration one needs to include the zero-mode contribution to solve the noncovariance problem. This amounts to performing the integration in a proper way in the covariant LFQM [27, 28]. In particular for $p'_{1\mu}$ and $\hat{p}'_{1\mu}p'_{1\nu}$ we have

$$\begin{aligned}\hat{p}'_{1\mu} &\doteq P_\mu A_1^{(1)} + q_\mu A_2^{(1)}, \hat{N}_2 \rightarrow Z_2, \\ \hat{p}'_{1\mu}\hat{p}'_{1\nu} &\doteq g_{\mu\nu}A_1^{(2)} + P_\mu P_\nu A_2^{(2)} + (P_\mu q_\nu + q_\mu P_\nu)A_3^{(2)} + q_\mu q_\nu A_4^{(2)},\end{aligned}\tag{A1}$$

with the symbol \doteq denoting that these equations are valid after integration. $A_j^{(i)}$ are functions of $x_{1,2}$, $p_\perp'^2$, $p_\perp' \cdot q_\perp$ and q^2

$$\begin{aligned}
Z_2 &= \hat{N}'_1 + m_1'^2 - m_2^2 + (1 - 2x_1)M'^2 + (q^2 + q \cdot P) \frac{p_\perp' \cdot q_\perp}{q^2}, \\
A_1^{(1)} &= \frac{x_1}{2}, \quad A_2^{(1)} = A_1^{(1)} - \frac{p_\perp' \cdot q_\perp}{q^2}, \quad A_1^{(2)} = -p_\perp'^2 - \frac{(p_\perp' \cdot q_\perp)^2}{q^2}, \\
A_3^{(2)} &= A_1^{(1)} A_2^{(1)}, \quad A_4^{(2)} = (A_2^{(1)})^2 - \frac{1}{q^2} A_1^{(2)}.
\end{aligned} \tag{A2}$$

-
- [1] B. Aubert *et al.* [BABAR Collaboration], Phys. Rev. Lett. **90**, 242001 (2003) [arXiv:hep-ex/0304021].
 - [2] D. Besson *et al.* [CLEO Collaboration], Phys. Rev. D **68**, 032002 (2003) [Erratum-ibid. D **75**, 119908 (2007)] [arXiv:hep-ex/0305100].
 - [3] F. De Fazio, arXiv:0910.0412 [hep-ph].
 - [4] A. V. Evdokimov *et al.* [SELEX Collaboration], Phys. Rev. Lett. **93**, 242001 (2004) [arXiv:hep-ex/0406045].
 - [5] K. Abe *et al.* [Belle Collaboration], arXiv:hep-ex/0608031.
 - [6] B. Aubert *et al.* [BABAR Collaboration], Phys. Rev. D **80**, 092003 (2009) [arXiv:0908.0806 [hep-ex]].
 - [7] B. Aubert *et al.* [BABAR Collaboration], Phys. Rev. Lett. **97**, 222001 (2006) [arXiv:hep-ex/0607082].
 - [8] P. Colangelo, F. De Fazio and S. Nicotri, Phys. Lett. B **642**, 48 (2006) [arXiv:hep-ph/0607245].
 - [9] B. Zhang, X. Liu, W. Z. Deng and S. L. Zhu, Eur. Phys. J. C **50**, 617 (2007) [arXiv:hep-ph/0609013].
 - [10] B. Chen, D. X. Wang and A. Zhang, Phys. Rev. D **80**, 071502 (2009) [arXiv:0908.3261 [hep-ph]].
 - [11] E. van Beveren and G. Rupp, Phys. Rev. D **81**, 118101 (2010) [arXiv:0908.1142 [hep-ph]].
 - [12] M. Di Pierro and E. Eichten, Phys. Rev. D **64**, 114004 (2001) [arXiv:hep-ph/0104208].
 - [13] T. Matsuki, T. Morii and K. Sudoh, Eur. Phys. J. A **31**, 701 (2007) [arXiv:hep-ph/0610186].
 - [14] D. Ebert, R. N. Faustov and V. O. Galkin, arXiv:0910.5612 [hep-ph].
 - [15] F. E. Close, C. E. Thomas, O. Lakhina and E. S. Swanson, Phys. Lett. B **647**, 159 (2007) [arXiv:hep-ph/0608139].
 - [16] G. L. Wang, Phys. Lett. B **650**, 15 (2007) [arXiv:0705.2621 [hep-ph]].
 - [17] P. Colangelo and F. De Fazio, Phys. Rev. D **81**, 094001 (2010) [arXiv:1001.1089 [hep-ph]].
 - [18] Z. F. Sun and X. Liu, Phys. Rev. D **80**, 074037 (2009) [arXiv:0909.1658 [hep-ph]].
 - [19] X. H. Zhong and Q. Zhao, Phys. Rev. D **81**, 014031 (2010) [arXiv:0911.1856 [hep-ph]].
 - [20] M. Artuso *et al.*, Eur. Phys. J. C **57**, 309 (2008) [arXiv:0801.1833 [hep-ph]]; N. Harnew, Phys. Atom. Nucl. **71**, 588 (2008).
 - [21] For example, see T. Aushev *et al.*, arXiv:1002.5012 [hep-ex]. The number of B_s^0 mesons is estimated to be $\sim 5.9 \times 10^8$ in the dataset of $L_{\text{int}} = 5ab^{-1}$ taken at the $\Upsilon(5S)$.
 - [22] M. Q. Huang, Phys. Rev. D **69**, 114015 (2004) [arXiv:hep-ph/0404032].
 - [23] S. M. Zhao, X. Liu and S. J. Li, Eur. Phys. J. C **51**, 601 (2007) [arXiv:hep-ph/0612008].
 - [24] T. M. Aliev and M. Savci, Phys. Rev. D **73**, 114010 (2006) [arXiv:hep-ph/0604002].
 - [25] T. M. Aliev, K. Azizi and A. Ozpineci, Eur. Phys. J. C **51**, 593 (2007) [arXiv:hep-ph/0608264].
 - [26] R. H. Li, C. D. Lu and Y. M. Wang, Phys. Rev. D **80**, 014005 (2009) [arXiv:0905.3259 [hep-ph]].
 - [27] W. Jaus, Phys. Rev. D **60**, 054026 (1999).
 - [28] H. Y. Cheng, C. K. Chua and C. W. Hwang, Phys. Rev. D **69**, 074025 (2004).
 - [29] H. Y. Cheng and C. K. Chua, Phys. Rev. D **69**, 094007 (2004) [arXiv:hep-ph/0401141].
 - [30] H. W. Ke, X. Q. Li and Z. T. Wei, Phys. Rev. D **80**, 074030 (2009) [arXiv:0907.5465 [hep-ph]].
 - [31] H. W. Ke, X. Q. Li and Z. T. Wei, arXiv:0912.4094 [hep-ph].
 - [32] H. Y. Cheng and C. K. Chua, Phys. Rev. D **81**, 114006 (2010) [arXiv:0909.4627 [hep-ph]].
 - [33] C. D. Lu, W. Wang and Z. T. Wei, Phys. Rev. D **76**, 014013 (2007) [arXiv:hep-ph/07011265]; W. Wang, Y. L. Shen and C. D. Lu, Eur. Phys. J. C **51**, 841 (2007) [arXiv:0704.2493 [hep-ph]]; W. Wang and Y. L. Shen, Phys. Rev. D **78**, 054002 (2008); Y. L. Shen and Y. M. Wang, Phys. Rev. D **78**, 074012 (2008); W. Wang, Y. L. Shen and C. D. Lu, Phys. Rev. D **79**, 054012 (2009) [arXiv:0811.3748 [hep-ph]]; X. X. Wang, W. Wang and C. D. Lu, Phys. Rev. D **79**, 114018 (2009) [arXiv:0901.1934 [hep-ph]]; C. H. Chen, Y. L. Shen and W. Wang, Phys. Lett. B **686**, 118 (2010) [arXiv:0911.2875 [hep-ph]]; W. Wang, arXiv:1002.3579 [hep-ph].
 - [34] For a review, see G. Buchalla, A. J. Buras and M. E. Lautenbacher, Rev. Mod. Phys. **68**, 1125 (1996) [arXiv:hep-ph/9512380].
 - [35] W. Jaus, Phys. Rev. D **41**, 3394 (1990).
 - [36] W. Jaus, Phys. Rev. D **44**, 2851 (1991).
 - [37] H. Y. Cheng, C. Y. Cheung and C. W. Hwang, Phys. Rev. D **55**, 1559 (1997) [arXiv:hep-ph/9607332].
 - [38] H. M. Choi, C. R. Ji and L. S. Kisslinger, Phys. Rev. D **65**, 074032 (2002) [arXiv:hep-ph/0110222].
 - [39] C. Amsler *et al.* [Particle Data Group], Phys. Lett. B **667**, 1 (2008); K. Nakamura *et al.* [Particle Data Group], J. Phys. G **37**, 075021 (2010).
 - [40] H. M. Choi, arXiv:hep-ph/9911271.

- [41] E. Gamiz, C. T. H. Davies, G. P. Lepage, J. Shigemitsu and M. Wingate [HPQCD Collaboration], Phys. Rev. D **80**, 014503 (2009) [arXiv:0902.1815 [hep-lat]].
- [42] Heavy-Flavor-Averaging-Group, http://www.slac.stanford.edu/xorg/hfag/charm/PIC09/f_ds/results.html.
- [43] A. Faessler, T. Gutsche, S. Kovalenko and V. E. Lyubovitskij, Phys. Rev. D **76**, 014003 (2007) [arXiv:0705.0892 [hep-ph]].
- [44] R. Louvot *et al.* [Belle Collaboration], Phys. Rev. Lett. **104**, 231801 (2010) [arXiv:1003.5312 [hep-ex]].
- [45] K. Kinoshita, arXiv:1005.3893 [hep-ex]; S. Esen *et al.* [Belle Collaboration], arXiv:1005.5177 [hep-ex].
- [46] M. Wirbel, B. Stech, M. Bauer, Z. Phys. C**29**, 637 (1985); M. Bauer, B. Stech, M. Wirbel, Z. Phys. C**34**, 103 (1987).
- [47] A. Ali and C. Greub, Phys. Rev. D**57**, 2996 (1998) [hep-ph/9707251]; G. Kramer, W. F. Palmer and H. Simma, Nucl. Phys. B**428**, 77 (1994); Z. Phys. C**66**, 429 (1995).
- [48] A. Ali, G. Kramer, and C. -D. Lü, Phys. Rev. D**58**, 094009 (1998) [hep-ph/9804363]; Phys. Rev. D**59**, 014005 (1999) [hep-ph/9805403]; Y. H. Chen, H. Y. Cheng, B. Tseng, and K. C. Yang, Phys. Rev. D**60**, 094014 (1999) [hep-ph/9903453].
- [49] C. W. Bauer, D. Pirjol and I. W. Stewart, Phys. Rev. Lett. **87**, 201806 (2001) [arXiv:hep-ph/0107002].
- [50] C. W. Bauer, S. Fleming, D. Pirjol and I. W. Stewart, Phys. Rev. D **63**, 114020 (2001) [arXiv:hep-ph/0011336].
- [51] P. Blasi, P. Colangelo, G. Nardulli and N. Paver, Phys. Rev. D **49**, 238 (1994) [arXiv:hep-ph/9307290].
- [52] J. M. Zhang and G. L. Wang, Chin. Phys. Lett. **27**, 051301 (2010) [arXiv:1003.5576 [hep-ph]].
- [53] A. Deandrea, N. Di Bartolomeo, R. Gatto and G. Nardulli, Phys. Lett. B **318**, 549 (1993) [arXiv:hep-ph/9308210].
- [54] R. H. Li, C. D. Lu and H. Zou, Phys. Rev. D **78**, 014018 (2008) [arXiv:0803.1073 [hep-ph]].
- [55] R. H. Li, X. X. Wang, A. I. Sanda and C. D. Lu, Phys. Rev. D **81**, 034006 (2010) [arXiv:0910.1424 [hep-ph]].